# Metal Nanoparticle Imaging with Photothermal Optical Coherence Tomography

***Yaguang Zeng, Dingan Han****

Department of photoelectric technology, Foshan University, Guangdong, 528000, China

E-mail: handingan@163.com

## Abstract

We demonstrate a method to use the photothermal phase difference to map metal nanoparticle (NP) agents with optical coherence tomography. The depth-resolved real time light-to-heat conversion can be traced by recording the photothermal phase. Under the condition of the adiabatic absorption, compared with phase modulation, the photothermal phase difference presents completely the light absorption information and has a speed advantage to reconstruct MNP agent distribution in phantoms and in mouse bladder *in vitro*.

## 1. Introduction

Recently, metal nanoparticle (MNP) has attracted wide interests in biomedical applications such as tumor labels, biological imaging agents and so on [1-4]. When an exciting laser hits MNP collective Plasmon resonance, MNP can absorb the light energy completely. As MNP has a very low optical quantum yield, the light energy mainly converts into heat, which simultaneously diffuses to the surrounding, causing the thermal expansion and the thermal refractive index effect. This results in the detectable change of the optical path and adds a photothermal phase for frequency domain optical coherence tomography (FD-OCT) [5,6]. The phase modulation technique of FD-OCT is used to obtain the depth-resolved amplitude of photothermal phase excited by the modulation laser. The method has been successfully demonstrated to map the contrast MNP agents in phantoms or biomedical tissues [5-6]. However, in order to obtain accurate Fourier transform and high signal-to-noise rate (SNR), hundreds of modulation cycles are required, which takes longer acquired time for image application. For example, in Ref [4], images were acquired with 1 second at each of lateral positions (1000 sequential A-scans and 1 ms integration time for each A-scan). Another disadvantage is that the resolved phase amplitude depends on not only the heat generation related to the light absorption, but also the heat relaxation determined by the environment. Generally speaking, the thermal decay time is longer than the ramp time for most samples. Thus, the resolved modulation phase amplitude can not completely present the light absorption information. In this paper, we propose a new method to map the MNP agent image by using the photothermal phase difference similar to traditional Doppler OCT. The method provides local complete light absorption message and has a speed advantage compared with the phase modulation.

## 2. Experimental results and discussion

We use a phantom and a mouse bladder in vitro for MNP agent imaging (shown in Fig. 1). Gold nanorods are made to MNP agents based on seed-mediated growth technique. They present an absorption peak of ~810 nm and have an aspect ratio of about 4.2 and a length of 50nm.The process for preparing the gold MNP has demonstrated in Ref. [10]. The FD-OCT experimental system is simply described in Fig.1 as follow: a superlumincent diode (SLD, dense light, DL-BX9-CS3307A) is used as the OCT light source with a central wavelength of 1310nm and a bandwidth of 5sss5 nm. It can provide an axial resolution of 13μm in air. An aiming source (λ=675nm) is coupled into the fiber to indicate the detected position. The max sampling frequency of the linear CCD is 47 KHz (Goodrich, SU-LDH). In the sample arm, the detecting laser beam and the pump laser with a wavelength of 808nm and a maximum output power of

978-1-4673-5225-3/14/$31.00 ©2014 IEEE

400mW are combined by using a dichroic mirror via a XY pair of scan mirrors. A computer is used to synchronously control a linear CCD and generate the square wave to trigger the pump laser.

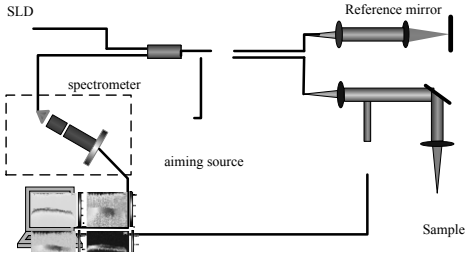


Fig.1 . Schematic of the FD-FD-OCTsystem used in this study

Firstly, we measure the photothermal phase of the MNP phantom by using M-scan to verify our theory. The experiment phantom is a mixture of agar 2g, gold MNP particle solution 10ml with the concentration 40ug/l and water 88ml. In our experiment, the sampling rate of the CCD is set 8.717 KHz (0.1ms integration time for each A-scan) and the total acquired time is 114.7ms corresponding to 1000 A-scan lines. The pump laser with output power 30mw is delayed 17.72ms to be triggered relative to the start time of the linear CCD. Fig.2 (a) shows the photothermal phase with the illumination duration 35.12ms corresponding to 300 A-scan lines. The blue, black and red lines show the trigger signal, the raw data profile of the recorded photothermal phase and the linear fitting profile. Fig.2 (a) shows the illumination location attends to reach a thermal equilibrium for the case of a longer illumination time. After

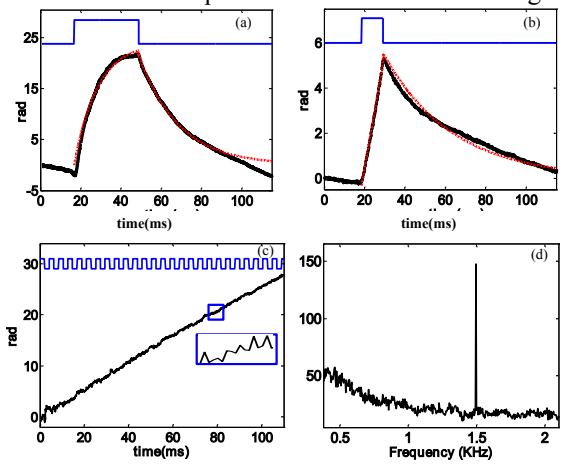


Fig.2: (a) Blue, black and red profiles indicate the trigger signal, the photothermal phase with pulse duration 35.12ms and the fitting profile; (b) Black and red profiles indicate the photothermal phase and their fitting profile with pulse duration 9.29ms; (c) the black profile indicates the photothermal phase excited by modulating laser (blue profile) with 1.5KHz, the slow phase component removed by subtracting a quadratic fit. (d) The amplitude spectrum of the recorded phase through Fast Fourier transforms

the light is turned off, the phase decays exponentially back. One can find that the fitting profile agree well with the raw data. Those results can prove that the photothermal phase is related to the temperature change. So the photothermal phase can trace the depth-resolved real time light-to-heat conversion. Fig. 2(b) presents the photothermal phase signal with the illumination time 9.29ms corresponding to 80 A-scan lines. The photothermal phase increases linearly for the case of the short illumination time. So the light absorption can be viewed as the adiabatic process and the photothermal phase difference can present the light absorption. Compared the increased phase departure with the decay phase departure shown in Figs. 2(a) and (b), we find that the heat relaxation takes longer time than the light absorption. In order to compare with the phase modulation, we also measure the photothermal phase of the phantom excited by the modulation laser with 1.5 KHz. Fig.2(c) shows the modulating photothermal phase (115ms,1024 A-scan lines). The slow phase component is removed by subtracting a quadratic fit in Fig.2(c), which shows the weak phase variation. Fig. 2(d) shows the amplitude spectrum of the recorded phase through the Fast

Fourier transform and the modulation phase signal at 1.5KHz. As we analyzed, since the heat relaxation takes more time than the light absorption, the modulating laser generates a continuous increasing background temperature. However, the phase modulation amplitude can not show the increasing background temperature because the increasing background temperature corresponds to DC part in frequency domain. So the phase modulation amplitude can not present completely the light absorption information.

Fig.3 shows the different concentration of MNP phantoms through the photothermal phase difference as the image parameter. Four cylindrical phantoms with the diameter 1.5mm are made (agar (2%), gold MNP particle solution (1% with the different concentration 0ug/l, 10ug/l, 20ug/l, and 40ug/l, respectively) and water (97%)), and put side by side on a glass plane. The sample with concentration 0ug/l is used as the

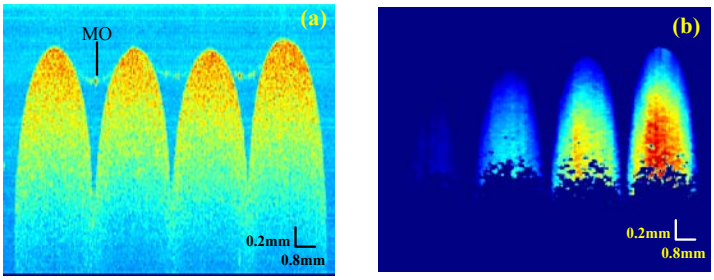


Fig.3: (a) Traditional OCT image of phantoms with different concentration (from the left to right 0ug/l, 10ug/l, 20ug/l, and 40ug/l, respectively); MO refers to the mineral oil layer; (b) photothermal phase difference image.

control sample, only the increased part of the phase is recorded. The total recorded time at every acquired position is 15.94ms corresponding to 140 A-scan lines. The exciting laser is delayed 4.52ms to be triggered and the illumination duration is $\tau_0 = 11.42ms$ corresponding to 100 A-scan lines. The average phase at the start 4.52ms is defined as the reference phase $\varphi(z,0)$. The photothermal phase $\varphi(z,\tau_0)$ is the average phase at the end of 20 A-scan lines (2.294ms). Based on upper experiment results in Fig.2 (b), the light absorption during 9.18ms is an adiabatic process. The photothermal phase difference is used as the imaging parameter. The 2D image was obtained to scan 200 lateral positions and take 15.94ms at every acquired position. In our experiment, the imaging speed is 63 times faster than the phase modulation. Phantoms in our experiment are covered with a mineral oil to avoid water evaporation during the experiment. Fig.3 (a) shows the traditional FD-OCT image of MNP phantoms, where the MNP concentrations from the left to right are 0ug/l, 10ug/l, 20ug/l, and 40ug/l, respectively. From these images, we find that there is no obvious difference among traditional FD-OCT images. It denotes that MNP does not affect the light scatter properties of phantoms. Fig.3(b) shows the photothermal phase difference images of these phantoms. As the mineral oil covers the top of the phantoms, the signal at the top of the phantoms is weaker than that at the bottom. The experiment result indicates the photothermal phase difference can distinguish the different concentration of MNP agent in phantoms.

Fig.4 presents the photothermal phase image of the mouse bladder *in vitro*. The experiment condition is same to above MNP phantoms. The mouse we used is three month-old male C57BL/6J mouse, and injected with MNP solution 20ml with the MNP concentration 60ug/l. After 2 hours, the bladder *in vitro* is used to reconstruct photothermal image. Using phase modulation, the MNP distribution in sentinel lymph nodes has demonstrated in Ref. (10). Fig.4 (a) shows the traditional FD-OCT image of the mouse bladder, where two layers can be distinguished from the structural position. The first layer at the surface is the detrusor muscle of the bladder and the second one is its muscularis mucosa, where they have nearly scatter intensity for the traditional OCT image. Fig.4 (b) shows the photothermal phase difference image of the bladder. We can find the two layers are very distinct intensity. The signal at the detrusor muscle layer is stronger than that of muscularis mucosa layer. The image shows the MNP is mainly deposited on the detrusor muscle layer. This result is reasonable because the muscularis mucosa layer is closed to the urinary inside the bladder. Fig.4 shows the photothermal phase difference has a potential application to map the MNP agent distribution in optical biomedicine.

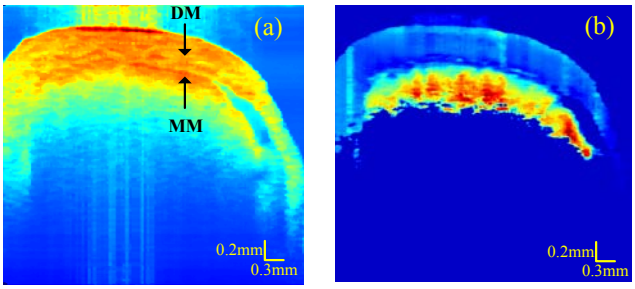


Fig.4: (a) Traditional OCT image of the mouse bladder, where DM and MM indicate the detrusor muscle and the muscularis mucosa of bladder, respectively; (b) Photothermal phase difference image of the mouse bladder.

Although our experiments give preliminary evidence that the photothermal phase difference can be used to reconstruct the light absorption and MNP distribution. However, there are many ways should be improved. In order to ensure that the light absorption is an adiabatic process and eliminate phase cumulative effect, the shorter excited square wave laser or pulse laser is required similar to the photoacoustic image. A feasible scheme is to record two A-scan lines at every position, where the first A-scan line records the reference phase and the second A-scan lines records the photothermal phase. Another problem is that the method is more sensitive to motion artifacts than the phase modulation, which will negatively impact the use of the method for in vivo imaging. Fortunately, there are many ways to eliminate the motion artifacts in FD-OCT, which has widely studied in blood flow perfusion.

## 4. Conclusion

In conclusion, we have demonstrated experimentally the photothermal phase can be used to trace the light absorption and the heat relaxation. Under the condition of adiabatic absorption, the photothermal phase difference can completely release the information of the local light absorption. It provides a speed advantage compared with the phase modulation method to image MNP agents in biological application.

## 5. References

1. T. Lee, A. Oldenburg, and S. Boppart, “Engineered microsphere contrast agents for optical coherence tomography,” *Opt. Lett.*, **28** 2003, pp. 1546-1548.

2. P. Yu, M. Mustata, and D. Nolte, “Holographic Optical Coherence Imaging of Rat Osteogenic Sarcoma TumorSpheroids,” *Appl. Opt.*, **43**, 2004, pp. 4862-4873.

3. L. Cognet, C. Tardin, P. Tamarat, and B. Lounis, “Singlemetallic nanoparticle imaging for protein detection in cells,” *PNAS*, **100**, 2003, pp. 11350–11355.

4. A. M. Gobin, R. A. Drezek, and J. L. West.“Near-Infrared Resonant Nanoshells for Combined Optical Imaging and Photothermal Cancer Therapy,” *Nano. Lett.*, **7** , 2007, pp.1929–1934 .

5. Y. Zeng, K. Xiong, X. Lu, G. Feng, D. Han, and J. Wu, “Laser Doppler projection tomography”, *Opt. Lett.*, **39**, 2014, pp.904-906.

6. M. Wang, Y. Zeng, X. and G. Yang, “Full-field optical micro-angiography”, *Appl. Phys. Lett.*, **104**, 2014, pp. 053704.